Further investigation on the dynamic compressive strength enhancement of concrete-like materials based on split Hopkinson pressure bar tests Part II Numerical Simulations

Q.M. Li, Y.B. Lu, H. Meng

Accepted Manuscript

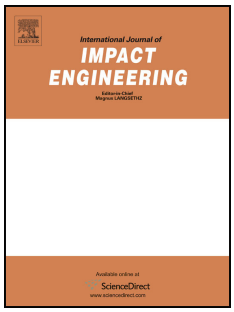

Title: Further investigation on the dynamic compressive strength enhancement of concrete-like materials based on split Hopkinson pressure bar tests Part II Numerical Simulations

Authors: Q.M. Li, Y.B. Lu, H. Meng

PII: S0734-743X(09)00096-7

DOI: 10.1016/j.ijimpeng.2009.04.010

Reference: IE 1783

To appear in: *International Journal of Impact Engineering*

Please cite this article as: Li QM, Lu YB, Meng H. Further investigation on the dynamic compressive strength enhancement of concrete-like materials based on split Hopkinson pressure bar tests Part II Numerical Simulations, International Journal of Impact Engineering (2009), doi: 10.1016/j.ijimpeng.2009.04.010

Further investigation on the dynamic compressive strength enhancement of concrete-like materials based on split Hopkinson pressure bar tests
Part II Numerical Simulations

Q.M.Li[1,2*], Y.B.Lu[1], H.Meng[3]

[1]School of Mechanical, Aerospace and Civil Engineering, Pariser Building
The University of Manchester, PO Box 88, Manchester M60 1QD, UK

[2]State Key Laboratory of Explosion Science and Technology
Beijing Institute of Technology, Beijing 100081, China

[3]Wuhan Construction Project Quality Supervision Station
Jianshe Road 721#, Wuhan 430015, China

Abstract: Split Hopkinson pressure bars (SHPB) have been used widely to measure the dynamic compressive strength of concrete-like materials at high strain-rate between 10^1 and 10^3 s^{-1}. It has been shown in companion paper (Zhang et al. 2009) that the axial strain acceleration is normally unavoidable in an SHPB test on brittle materials. Axial strain acceleration introduces radial confinement in the SHPB specimens and consequently enhances the compressive strength of concrete-like specimens. This paper employs numerical simulation to further demonstrate that the unexpected radial confinement in an SHPB test is responsible for the increase of the dynamic compressive strength of concrete-like materials at strain rates from 10^1 to 10^3 s^{-1}. It confirms the observations in Zhang et al. (2009) that the dynamic increase factor (DIF) measured in SHPB tests can be reduced either by using tubular SHPB specimens or by reducing the diameter of the SHPB specimen. A kinetic friction model is proposed based on kinetic friction tests and is implemented in the numerical model. It shows that it is necessary to use a kinetic friction model, rather than a constant friction model, for more accurate numerical simulation of SHPB tests.

Keywords: concrete-like materials, split Hopkinson pressure bar, dynamic increase factor, compressive strength, kinetic friction model, numerical simulation

*Corresponding author and guest professor to Beijing Institute of Technology
E-mail: qingming.li@manchester.ac.uk

1 Introduction

Strain-rate effects on the compressive strength of various concrete-like materials, e.g., concrete, mortar, rock etc, have become an important consideration in the material strength model in numerical analysis and design of the protective structures made from concrete-like materials. It is generally accepted that the dynamic compressive strength of concrete-like materials increases with strain-rate, which is represented by a dynamic increase factor (DIF) defined by the ratio of the dynamic strength to the quasi-static strength in unconfined uniaxial compression.

A great number of tests have been performed to find the dependence of DIF on strain-rate using various test methods, e.g., drop-hammer techniques, servo-hydraulic loading rigs, explosive devices and split Hopkinson pressure bar (SHPB) technique. Critical reviews were conducted by Bischoff and Perry (1991) and Williams (1994), where the DIF of concrete based on various experimental techniques was summarized. In past two decades, the SHPB technique, which was developed originally to measure the dynamic flow stress-strain relations of plastic materials, has been applied to determine the dynamic compressive strength of brittle materials in a wide range of strain-rates between 10^1 and 10^3 s^{-1}.

It has been realized that radial inertia effects are associated with the unavoidable axial strain acceleration (i.e. $\ddot{\varepsilon}_z = d\dot{\varepsilon}/dt \neq 0$) in an SHPB test (Kolsky 1949; Davies and Hunter 1963; Haddow 1965; Samanta 1971; Gorham 1989, 1991; Gorham et al. 1984, 1992), which leads to radial confinement pressure in the SHPB specimen. Based on the equations of radial confinement pressure derived in these studies, it was found that the effect of radial inertia is proportional to the square of the specimen diameter. Therefore, these researchers pointed out that specimens used for high strain-rate testing should be as small as possible to avoid radial inertia effects. An expression of the radial stress distribution in a solid elastic cylindrical specimen subjected to axial strain acceleration $\ddot{\varepsilon}_z(t)$ can be expressed as a quadratic function of radius, i.e. (Forrestal et al., 2007)

$$\sigma_r = -\frac{\nu(3-2\nu)}{8(1-\nu)}\rho\ddot{\varepsilon}_z(t)(r^2 - \frac{1}{4}d_0^2) \tag{1}$$

in which ν and ρ are Poisson's ratio and density of the specimen material, r and d_0 are the radial coordinate and the outer diameter of the specimen.

It was found by Zhang et al. (2009) that the strain-rate at the moment of failure of the specimen in a SHPB test is closely correlated to the axial strain acceleration for both solid and tubular mortar specimens. Moreover, it was shown that the axial strain acceleration in a large-diameter solid specimen is greater than that in a small-diameter specimen while the axial

strain acceleration in a solid specimen is greater than that in a tubular specimen when they have the same outer diameter. Consequently, the radial confinement induced by the axial strain acceleration can be reduced by reducing the SHPB specimen diameter or by the use of tubular SHPB specimen (Zhang et al. 2009).

Brace and Jones (1971) found that the rapid increase of compressive strength of rocks after a transition strain-rate can be interpreted by the change of stress state from uniaxial stress to uniaxial strain, representing increased radial confinement (Field et al. 2004). It has also been shown in Li and Meng (2003) that the enhancement of the compressive strength of mortar due to the radial confinement in an SHPB test is often mistakenly interpreted as the strain-rate effect on the uniaxial compressive strength, leading to incorrect DIF formulae. These false DIF formulae, represented by CEB formulae (Comite Euro-International du Beton 1993), have been applied widely in the design and analysis of concrete structures against impact and blast loads. Thus, it is necessary to quantify the dynamic compressive strength enhancement due to the radial inertia confinement, especially when large-diameter specimens and high strain-rates are involved in an SHPB test.

The objective of the present study is to further investigate the influence of inertia-induced radial confinement on the determination of DIF in SHPB tests for concrete-like materials. Based on a finite element SHPB model, numerical SHPB tests are performed for a range of available SHPB testing results and parametric analyses. It reveals that currently-used DIF formulae based on SHPB tests greatly over-estimate the dynamic compressive strength of concrete-like materials at strain-rates between 10^1 and 10^3 s^{-1} due to the significant contributions from inertia-induced radial confinement.

2 Numerical SHPB experiment based on FEA

2.1 DIF of concrete-like material using SHPB technique

The increase of the dynamic compressive strength in concrete was first observed by Abrams (1917) and it has been generally accepted that the uniaxial compressive strength of a concrete-like material is strain-rate sensitive and the strength model of such materials should include strain-rate effects. A wide range of concrete and cement mortar with different quasi-static strengths (f_{cs}) have been tested in laboratories in order to quantify strain-rate effects (Fu et al. 1991a, b; Bischoff and Perry 1991), showing an obvious strength enhancement at strain-rates above a critical value between 10^1 and 10^2 s^{-1} (Malvern and Ross 1985; Tedesco and Ross 1998; Grote et al. 2001). Some publications of SHPB experimental results on concrete and mortar are discussed in this section.

European CEB recommended a DIF formula for concrete in compression (Comite Euro-International du Beton 1993), which takes the following form

$$DIF = \frac{f_{cd}}{f_{cs}} = \begin{cases} (\dot{\varepsilon} / \dot{\varepsilon}_s)^{1.026\alpha_s} & \dot{\varepsilon} \le 30s^{-1} \\ \gamma_s (\dot{\varepsilon} / \dot{\varepsilon}_s)^{0.33} & \dot{\varepsilon} > 30s^{-1} \end{cases} \tag{2}$$

where f_{cs} and f_{cd} are the unconfined uniaxial compressive strength in quasi-static and dynamic loading, respectively. $\gamma_s = 10^{(6.156\alpha_s - 2)}$, $\alpha_s = 1/(5 + 9 f_{cs} / f_{co})$, $\dot{\varepsilon}_s = 3 \times 10^{-5}$ s^{-1} and $f_{co} = 10$ MPa. Figure 1 depicts the CEB formula when f_{cs} =40 MPa is used in Eq.(2), which fits the SHPB test results of Malvern and Ross (1985), as verified by Bischoff and Perry (1991).

Based on SHPB results on concrete with different strengths and moistures (Ross et al. 1989, 1995, 1996; Tedesco and Ross 1998), a DIF regression equation was suggested by Tedesco and Ross (1998), i.e.

$$DIF = \begin{cases} 1 + 0.00965(\lg \dot{\varepsilon} + 6) \ge 1 & \dot{\varepsilon} \le 63.1s^{-1} \\ 1 + 0.758(\lg \dot{\varepsilon} - 0.938) \le 2.5 & \dot{\varepsilon} > 63.1s^{-1} \end{cases} \tag{3}$$

in which the transition from a low strain-rate-sensitivity to high strain-rate-sensitivity occurs at a critical strain-rate of 63.1 s^{-1}, which is slightly higher than the transition strain-rate given by the CEB formula in Eq.(2).

Grote et al. (2001) gave a formula to measure the DIF of mortar obtained by SHPB tests in the strain-rate range of 250~1700 s^{-1}, i.e.

$$DIF = \begin{cases} 1 + 0.0235(\lg \dot{\varepsilon} + 2.979) & \dot{\varepsilon} \le 266s^{-1} \\ 0.882(\lg \dot{\varepsilon})^3 - 4.4(\lg \dot{\varepsilon})^2 + 7.22 \lg \dot{\varepsilon} - 2.64 & \dot{\varepsilon} > 266s^{-1} \end{cases}, \tag{4}$$

with a transition strain-rate of 266 s^{-1}. It is found that Eq.(4) is not continuous at the transition strain-rate, as shown in Fig.1, when the DIF expression changes from a linear equation to a cubic equation. This discontinuity is overcome by a new data fitting expression using linear and quadratic equations, as shown in Eq.(5) and Fig.2,

$$DIF = \begin{cases} 1 + 0.0157(\lg \dot{\varepsilon} + 3) & \dot{\varepsilon} \le 266s^{-1} \\ 0.383 \lg^2 \dot{\varepsilon} + 0.226 \lg \dot{\varepsilon} - 1.765 & \dot{\varepsilon} > 266s^{-1} \end{cases}. \tag{5}$$

Based on the numerical results of mortar for three different slenderness ratios (i.e. length-to-diameter ratios), a relation between DIF and logarithm strain-rate was suggested by Li and Meng (2003)

$$DIF = \begin{cases} 1 + A_1(\lg \dot{\varepsilon} + A_2) & \dot{\varepsilon} \le 10^2 s^{-1} \\ A_3 \lg^2 \dot{\varepsilon} + A_4 \lg \dot{\varepsilon} + A_5 & \dot{\varepsilon} > 10^2 s^{-1} \end{cases}, \tag{6}$$

where A_1=0.0344, A_2=3.0, A_3=1.729, A_4=-7.137, A_5=8.530 are determined by Li and Meng (2003) using the least-squares method. They defined 10^{-4} s^{-1} as the quasi-static strain rate, but the value of the DIF becomes one when the strain rate is 10^{-3} s^{-1} according to Eq.(6), which leads to a local drop at the transition strain-rate, as shown in Fig.1. This abnormality can be eliminated by changing the values of A_1 and A_2 to 0.0258 and 4.0, as shown in Fig.2.

Many DIF formulae based on SHPB results (e.g. Comite Euro-International du Beton 1993; Tedesco and Ross 1998; Grote et al. 2001) suggested that there exists a transition strain-rate, beyond which the DIF increases with strain-rate rapidly, as shown in Fig.1. Li and Meng (2003) clearly pointed out that the rapid increase of DIF with strain-rate beyond this transition point is mainly due to the increased radial confinement effect, rather than real strain-rate effect, on the compressive strength of the tested concrete or mortar specimens. This point of view will be further enhanced in the present investigation.

Generally, a relation between DIF and the strain-rate is insensitive to f_{cs} since DIF is a non-dimensional parameter, which is also supported by both Eq.(2) where the DIF decreases slightly with the increase of f_{cs} if the change of f_{cs} is not large, and the experimental results in Fig.17 in Zhang et al. (2009). The unconfined uniaxial compressive strength of mortar specimens is f_{cs}=44.90 MPa in Zhang et al.(2009), which is close to the f_{cs} values used in Li and Meng (2003) and Grote et al. (2001), where f_{cs} is 40.00 MPa and 46.05 MPa, respectively.

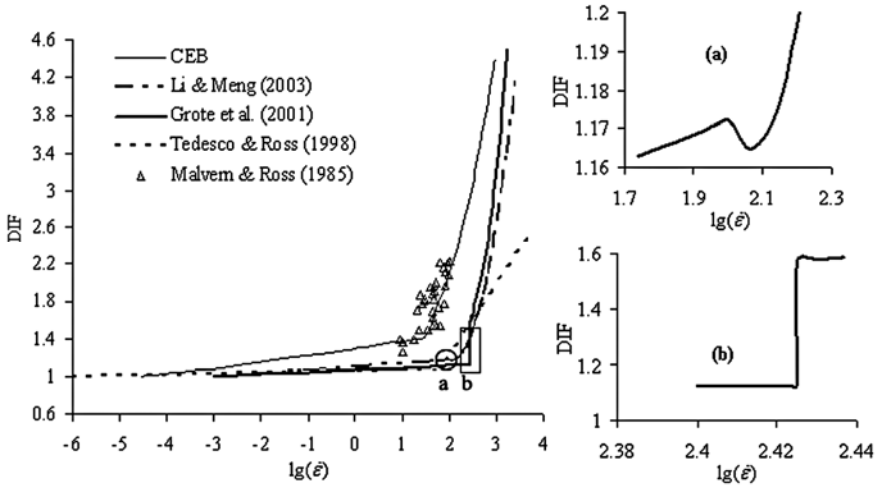

Fig.1. Various DIF recommendations where (a) and (b) are locally-enlarged curves of Li and Meng (2003) and Grote et al. (2001), respectively.

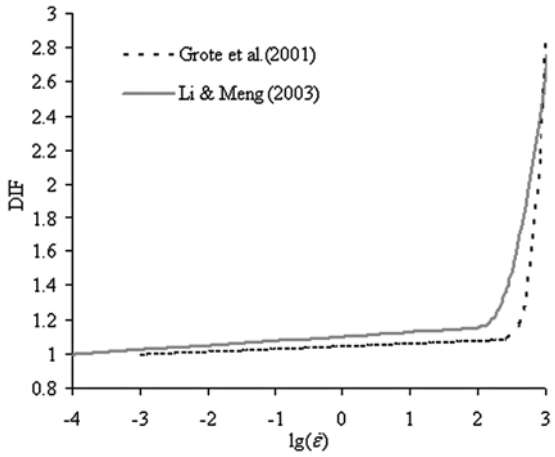

Fig.2. Corrected expressions of DIF formulae given by Grote et al. (2001) and Li & Meng (2003).

2.2 Methodology

In order to investigate the non-strain-rate effects on the compressive strength of concrete-like materials in an SHPB test, the strength model of the concrete-like material is initially assumed to be strain-rate insensitive. A quasi-static constitutive equation and a strength model are used in the numerical simulation of the tested SHPB specimen. The SHPB specimen and pressure bars are simulated as a structural problem to obtain a 'reconstituted' axial stress-strain relation, whose deviation from the input axial stress-strain curve indicates the error due to the violation of the fundamental assumptions in an SHPB test. This so-called 'reconstitution method' has been adopted by some researchers, e.g., Bertholf and Karnes (1975), Meng and Li (2003) and Li and Meng (2003). The advantage of using a strain-rate-independent stress-strain input curve is that all discrepancies between the 'reconstituted' stress-strain curve and the input stress-strain curve are not due to the strain-rate effect, but due to other factors, which should be correctly interpreted in the analyses of the SHPB test results. Further discussion on the 'reconstitution method' is given in Meng and Li (2003) and Li and Meng (2003).

2.3 Constitutive equation of mortar

A simplified uniaxial stress-strain relation of mortar is shown in Fig.3. A linear stress-strain relation is assumed between the ultimate tensile strength (f_{ts}) and the ultimate compression strength (f_{cs}), which is followed by a strain softening phase and a residual strength phase. The identification of a constitutive model for concrete-like materials requires test results from a uniaxial stress-strain relation and its dependence on the stress triaxiality.

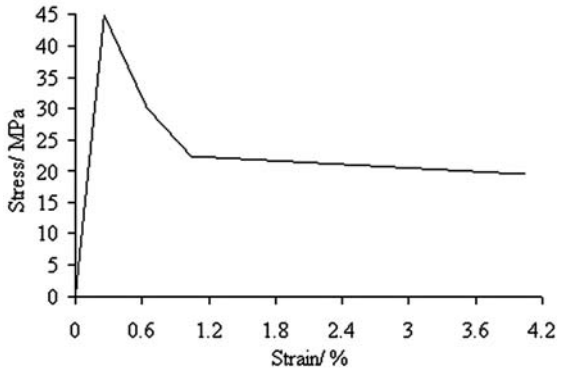

Fig.3. Quasi-static uniaxial compressive stress-strain curve of mortar (Li and Meng 2003).

To include the above mentioned features of concrete-like materials, various material models have been proposed, e.g., the plasticity concrete model in LS-DYNA (Malvar et al. 1997), the Drucker-Prager model in ABAQUS (Park et al. 2001; Li and Meng 2003), the hypoelastic model in ADINA (Tedesco et al. 1997). Among these models, the extended Drucker-Prager model is preferred since it is capable of providing a phenomenological account for the pressure-dependent flow due to the internal friction, which is a typical feature of concrete-like materials, and allows both the strain hardening and strain softening to be considered in the deformation up to material failure. More advanced constitutive models introduce more material parameters and increase computational difficulties and inaccuracy compared with a simplified model. Although the macroscopic deformation of concrete-like materials under compression-dominated stress state behaves like plastic deformation, it should be noted that the actual deformation mechanism of concrete beyond elastic regime is associated with the development of micro- and macro-cracks.

The yield function in a linear Drucker-Prager model is given by

$$F = t - p\tan\beta - d = 0 \tag{7}$$

where t is a pseudo-effective stress defined by $t = \frac{q}{2}[1 + \frac{1}{K} - (1 - \frac{1}{K})(\frac{r}{q})^3]$, $q = \sqrt{3J_2}$, $r^3 = \frac{27}{2}J_3$ with J_2 and J_3 being the second and third invariants of the deviatoric part of the Cauchy stress, the hydrostatic pressure $p = -I_1/3$ with I_1 being the first stress invariant, β is the slope of the linear yield surface in the p-t stress plane, the cohesion of the material $d = (1 - \frac{1}{3}\tan\beta)\sigma_c$ where σ_c is the uniaxial compression yield stress. K is the ratio between tensile and compressive triaxial strengths, which is in the range of 0.778~1 (ABAQUS 2004).

Park et al. (2001) showed that the response of mortar specimens is insensitive to K, and thus K=1 is used in this work.

The flow rule of the linear Drucker-Prager model is defined as

$$d\varepsilon^p = \frac{d\bar{\varepsilon}^p}{c}\frac{\partial G}{\partial \sigma} \tag{8}$$

where $c = 1 - \frac{1}{3}\tan\psi$ if hardening or softening is defined in uniaxial compression, $\bar{\varepsilon}^p$ is the equivalent plastic strain, and G is the flow potential, chosen in this model as

$$G = t - p\tan\psi \tag{9}$$

in which ψ is the dilation angle in the p-t plane. A geometric interpretation of ψ is shown in Fig.4.

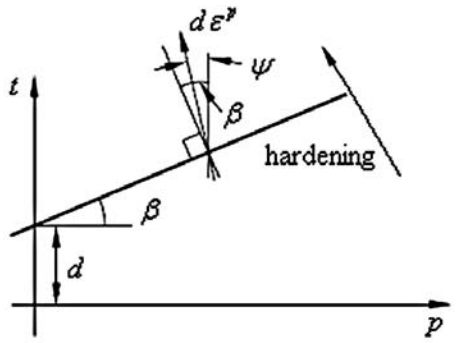

Fig.4. Yield surface and flow direction in the p-t plane.

Based on the data of actual triaxial compression tests (Dahl 1992; Zhang 2001), the values of β for mortar are in the range between 40° to 60°. The actual value of β for the mortar used in this study is not available. However, a parametric analysis suggests that simulations based on β=40° give the best agreement with SHPB experimental data for different dimensions of SHPB specimens in Zhang et al. (2009). Therefore, β=40° was used in the numerical simulations in the present study. Park et al. (2001) found that ψ has limited influence on the specimen response in their simulation of plate impact of mortar. It is further proved that the influence of ψ on DIF in a SHPB test is almost negligible according to parametric studies in the present research. Thus, a fully associated flow law, i.e. $\psi = \beta$, is used in the following simulations.

2.4 Numerical model

A description of the problem under consideration is illustrated in Fig.5, where the dimensions of the SHPB set-up are nearly the same as those used by Zhang et al. (2009) for the purpose of comparison. The specimens are made of mortar which was a mixture of cement, water and medium fine sand with mass proportion of 533:302:1600. Specimens with different ratios of inner to outer diameter, i.e., $d_i / d_o = 0$, 0.2, 0.4, 0.6, and various slenderness ratios in the range of 0.3~1.0 are used in the simulation of SHPB tests in the present study.

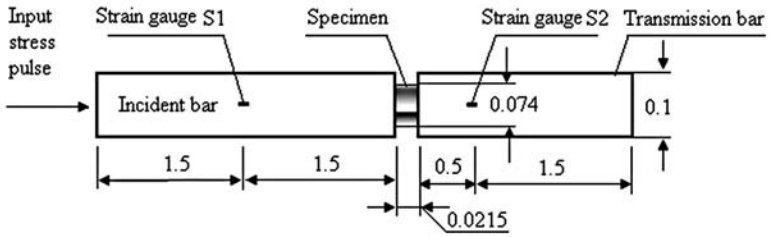

Fig.5. Configuration of the SHPB set-up for numerical simulation (the unit is meter).

Table 1 Material properties of SHPB and mortar sample

	Material	E / GPa	ρ / kg/m^3	ν
Pressure bar	Steel	200	7800	0.35
Specimen	Mortar	17.2	2179.0	0.19

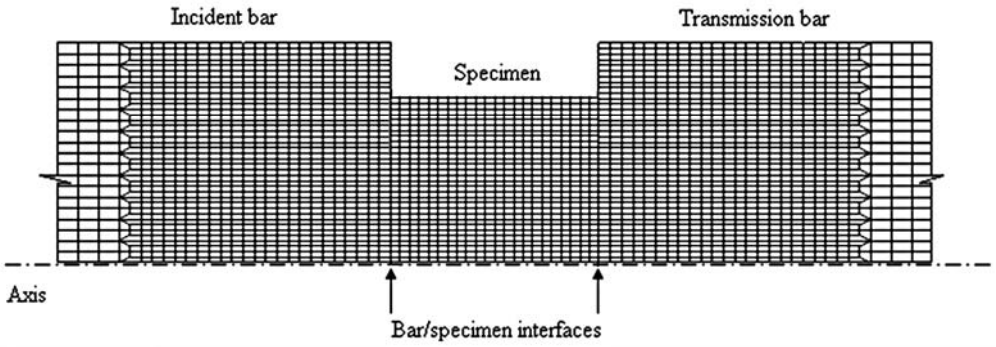

Fig.6. Axisymmetric finite element model of the specimen and the pressure bars.

The material properties of the SHPB apparatus and mortar specimen employed in the present study are taken from material tests on specimens with outer diameter of 74 mm in Zhang et al. (2009), as shown in Table 1, which are slightly different from those on SHPB specimens with outer diameters of 37 mm and 50 mm. Since numerical simulations are presented in non-dimensional quantities, it is not expected that the observed differences of their mechanical properties would influence the simulation results. Meanwhile, the numerical

simulations using the same values for the mechanical properties of the mortar specimen focuses on the influence of the geometries of the SHPB specimen on the DIF measured in SHPB tests. It should be noted that the conclusions obtained in this study are applicable to other conventional SHPB configurations and similar concrete-like materials.

ABAQUS/Explicit version 6.5-4 with element type CAX4R (axis symmetric element, reduced integration) is used for the calculations. The results based on the current mesh (as shown in Fig.6) are compared with those obtained for finer meshes in several trial simulations and the differences between them are insignificant. The contact between the specimen and the pressure bars is assumed to be frictionless and sliding is permitted. Further discussion about the influence of friction model on the SHPB testing results will be presented in Section 3.5.

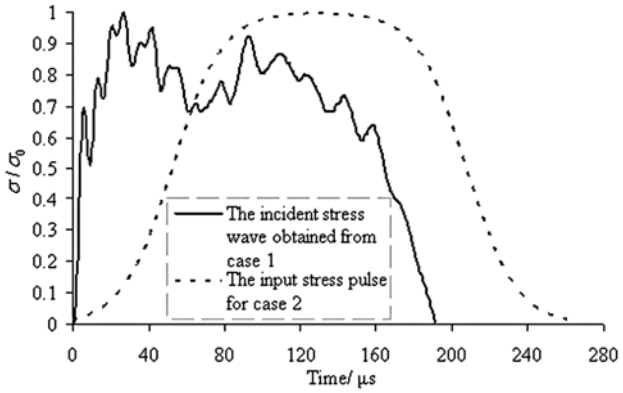

Fig.7. Incident stress pulses in two different cases.

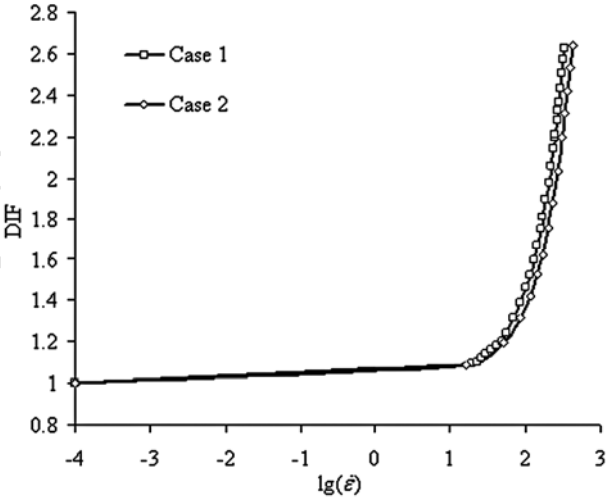

Fig.8. DIF versus strain-rate relationships under different shapes of stress pulse for solid specimens with outer diameter of 74 mm.

3 Results and discussion

3.1 The influence of stress pulse shape on DIF

The collision between a striker bar and an incident bar produces a stress pulse. The rise time of the pulse can be increased by properly choosing the material and dimensions of the wave shaper attached to the impact side of the incident bar. The amplitude and duration of the pulse depend mainly on the impact velocity and length of the striker bar, respectively. Furthermore, the actual shape of the pulse will be changed by the time it reaches the specimen due to wave dispersion. To investigate the influence of the pulse shape on the DIF, two cases are studied in this paper, as shown in Fig.7. The first assumes that the striker bar impacts the incident bar directly without a wave shaper in the numerical SHPB tests, and the second uses incident stress pulses described in Eqs.(2-3) in the companion paper (Zhang et al. 2009) with stress levels σ_0 varying from 39.5 to 552.9 MPa. This stress pulse replaces the actual impact between the striker bar and the incident pressure bar and is applied uniformly to the impact end face of the incident pressure bar. A comparison of the DIF results obtained from these two cases is shown in Fig.8. It is observed that the DIF measured from a numerical SHPB test decreases slightly with the rise time of the input pulse at the same strain rate. Therefore, instead of modeling the striker bar and a wave shaper, the empirical stress pulse given in Zhang et al. (2009) will be inputted into the incident pressure bar in the following numerical simulations in order to simplify the numerical model and save computational time.

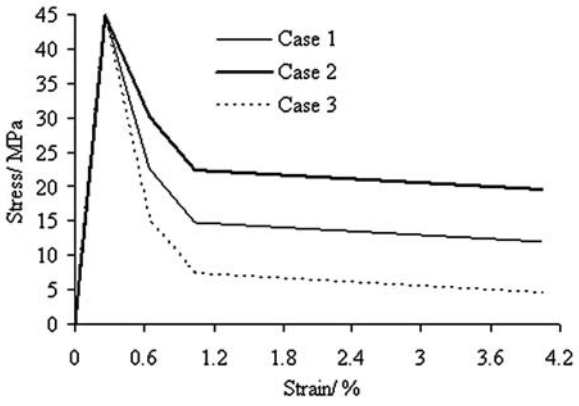

Fig.9. Unconfined uniaxial compression stress-strain relation with various residual strengths.

3.2 The influence of residual strength of mortar model on DIF

The uniaxial quasi-static stress-strain curve of the mortar specimen, which is simplified from the stress-strain relation in Maher and Darwin (1980), consists of a linear elastic relation with the ultimate compressive strength of 44.90 MPa and a strain softening region, as shown in Fig.3. Although the main concern of the present study is the ultimate uniaxial compressive strength of the SHPB specimen rather than the post-failure process in an SHPB test, some

elements in the SHPB specimen may enter into the post failure stage before the overall failure of the whole specimen. Therefore, three input curves with different residual strength shown in Fig.9 are adopted for the numerical SHPB simulations of mortar specimens in this paper. Figure 10 shows that the post-failure strength has negligible effect on the DIF around the transition strain-rate.

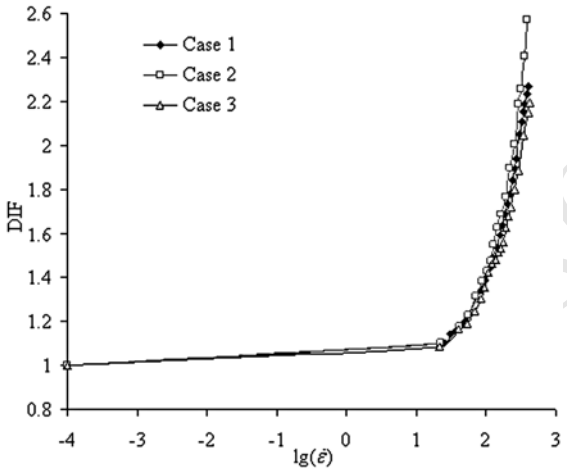

Fig.10. variations of DIF with logarithm strain-rate for different residual strengths.

3.3 The effect of slenderness ratio on DIF

Davies and Hunter (1963) gave an approximation of the contribution of axial strain acceleration to the additional axial stress as follows,

$$\sigma_z = \rho(\frac{1}{6}l_0^2 - \frac{1}{8}\nu^2 d_0^2)\ddot{\varepsilon}_z \tag{10}$$

where l_0 and d_0 are the original length and outer diameter of the specimen. Based on this expression, Davies and Hunter (1963) suggested that there exists an optimal slenderness ratio to minimize the influence of the inertial stress on the accuracy of an SHPB test, which takes the following form

$$\lambda_s = \frac{l_0}{d_0} = \frac{1}{2}\sqrt{3\nu} \ . \tag{11}$$

Equation (11) has been widely adopted as the optimal slenderness ratio for metallic SHPB specimens. Meanwhile, it has been extended to determine the slenderness ratio of non-metallic specimens in SHPB tests. However, this criterion of specimen geometry applies only if stress is measured by the transmitted pulse, as shown by Gorham et al. (1984, 1992) and Gorham (1989). Otherwise, when the stress in the specimen is calculated from the average of stresses on the two interfaces between the specimen and the pressure bars, the additional axial stress due to axial strain acceleration is

$$\sigma_z = \rho(\frac{l_0^2}{12} + \frac{d_0^2}{32})\ddot{\varepsilon}_z \qquad (12)$$

if the specimen is assumed to be incompressible. It is observed that both inertia terms on the right side of Eq.(12) are positive. In this instance, there is no specimen aspect ratio which could cause effective cancellation of inertia terms, and therefore, it is not valid to apply the optimal slenderness ratio in Eq.(11) to this situation.

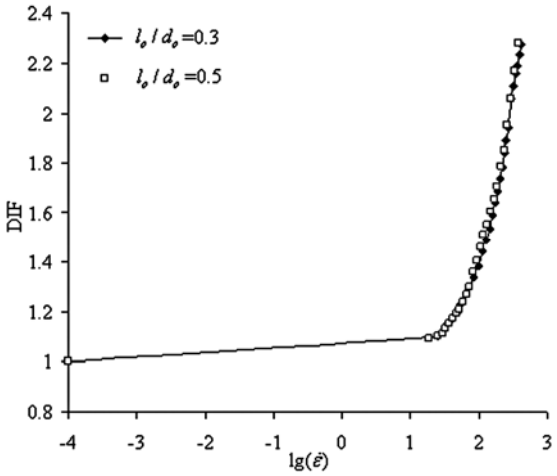

Fig.11. Influence of the slenderness ratio on DIF of tubular mortar specimens.

For concrete-like materials, ν is about 0.19, and thus the optimal slenderness ratio determined by Eq.(11) is 0.38. Relations between DIF and strain-rate for tubular mortar specimens (d_0 =74 mm and d_i =30.9 mm, where d_i is the inner diameter) with different slenderness ratios are shown in Fig.11. It is observed that the discrepancy in the relationship between DIF and strain rate is insignificant when $0.3 \le \lambda_s \le 1.0$ within the examined values of strain-rates in the present study. Similar observations are also reported by Li and Meng (2003) where solid mortar specimens with outer diameter of 12 mm and slenderness ratio λ_s varying from 0.3 to 1.0 were modelled in numerical SHPB tests. When λ_s <0.2, the uniaxial stress state no longer holds and inertia-induced radial confinement becomes an important factor for the enhancement of compressive strength, which agrees with the finding in Dioh et al.(1993) that a very different dependence of the apparent dynamic compressive strength on strain-rate appears when $\lambda_s < 0.2$. Besides, the influence of friction between an SHPB specimen and the pressure bars increases with the decrease of λ_s (i.e. flat SHPB specimens), which may also enhance the radial confinement (Meng and Li 2003). On the other hand, the axial inertia effect becomes important when $\lambda_s > 1.0$, which results in stress oscillations of the 'reconstituted'

stress-strain curves. The observed stress oscillation is caused by wave reflection between the two ends of the specimen before the uniform stress is achieved along the specimen (Meng and Li 2003).

3.4 The DIF of solid and tubular mortar specimens

As axial strain acceleration has great influence on the radial stress distribution in cylindrical specimens (Forrestal et al. 2007), the radial confinement induced by the axial strain acceleration should be considered (Zhang et al. 2009). It is observed that tubular and solid mortar specimens with the same outer diameter have nearly the same relationships between the axial strain acceleration and the strain rate (Zhang et al. 2009). However, the overall radial stress distribution in a tubular specimen is lower than that in a solid specimen induced by the same axial strain acceleration, which means that the radial confinement in a tubular specimen is smaller than that in a corresponding solid specimen. Therefore, the DIF from SHPB tests on tubular specimens is smaller than the DIF obtained from SHPB tests on solid specimens.

Figure 12 presents simulated variations of DIF with strain rates for solid and tubular mortar specimens of 74 mm in outer diameter. SHPB test results of tubular samples from Zhang et al. (2009) are also presented for comparison purpose. It is interesting to find that the DIFs of tubular specimens are consistently lower than those of solid specimens at the same strain-rate, and DIFs obtained from SHPB testing results reasonably follow the predicted DIFs from numerical simulations. Figure 12 shows the existence of inertia-induced radial confinement in SHPB tests of concrete-like materials.

It has been shown in Zhang et al.(2009) that the axial strain acceleration in large diameter solid specimens is greater than that in small ones at the same strain-rate in SHPB tests, which was discussed in Field et al.(2004) based on the transition from one-dimensional stress to one-dimensional strain states. According to Eq.(1), the radial stress increases with axial strain acceleration and the squares of the diameter of the SHPB specimen. Therefore, the radial confinement induced by the accelerated axial compression in large diameter SHPB specimens has greater influence on DIF than that in small diameter SHPB samples, which is verified by the comparison of DIF variations with strain-rates for solid specimens with different diameters, as shown in Fig.13. It is evident that DIFs for SHPB specimens with smaller diameters in Li and Meng (2003) (12 mm) and Grote et al. (2001) (10.1~18.8 mm) are smaller than DIFs for larger SHPB specimens (37~74 mm) in the present simulation and other SHPB results in Fig.13.

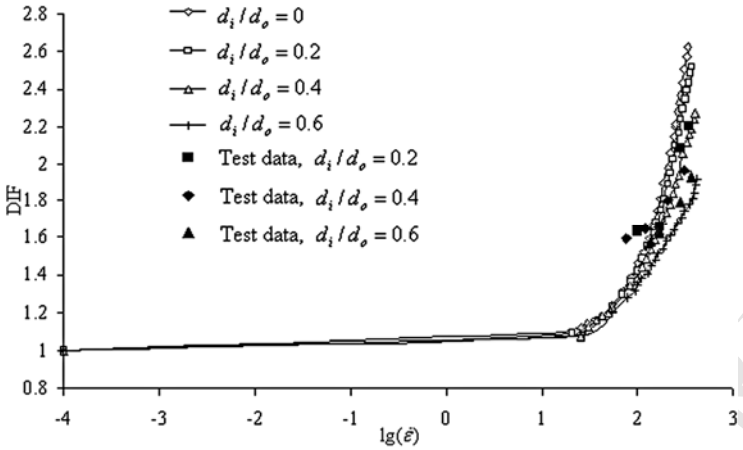

Fig.12. DIF versus strain-rate for solid and tubular mortar specimens with outer diameter of 74 mm.

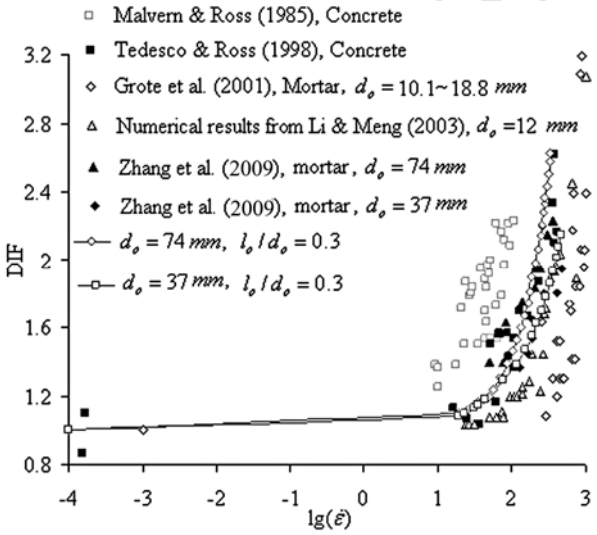

Fig.13. Comparison between the predicted DIF and experimental DIFs for mortar specimens from publications.

According to Fig.14, the apparent ultimate compressive strength starts to increase rapidly beyond a transition strain-rate around 22.9 s^{-1}. Defining 10^{-4} s^{-1} as the quasi-static strain-rate, all the numerical results for different specimen dimensions can be described by the following linear and quadratic equation of the logarithm strain-rate

$$DIF = \begin{cases} 1 + B_1(\lg\dot{\varepsilon} + B_2) & \dot{\varepsilon} \le 22.9s^{-1} \\ B_3\lg^2\dot{\varepsilon} + B_4\lg\dot{\varepsilon} + B_5 & \dot{\varepsilon} > 22.9s^{-1} \end{cases} \quad (13)$$

in the same form of Eq.(6), but with a different transition strain-rate $\dot{\varepsilon}_t$. Parameters in Eq.(13) for different outer diameters of solid mortar specimens are shown in Table 2. It should be

noted that there is a general scarcity of reliable experimental DIF data for concrete-like materials at strain-rates between 10^0 s^{-1} and 5×10^1 s^{-1}. When $\dot{\varepsilon} < 1.0$ s^{-1}, servo-hydraulic testing machines are usually used to test concrete-like materials. On the other hand, at high strain-rates between 5×10^1 and 10^3 s^{-1}, SHPBs are usually adopted. However, the lower limit of SHPB technique for testing concrete-like materials is in the strain-rate range of 10~100 s^{-1}. Accordingly, the general scarcity of reliable experimental data in the literature in this strain-rate range results in difficulties in determining the transition strain-rate accurately, as shown in Fig.13.

Comparison of Eq.(13) with Grote et al. (2001)'s recommendation and Li and Meng (2003)'s recommendation is illustrated in Fig.14. It shows that Eq.(13) is capable of describing apparent DIF dependence on strain-rates between 10^{-4} and 10^3 s^{-1} based on SHPB tests in spite of the unconfined uniaxial compressive strength of concrete-like materials although parameters in Table 2 depend on the outer diameters of the SHPB specimen.

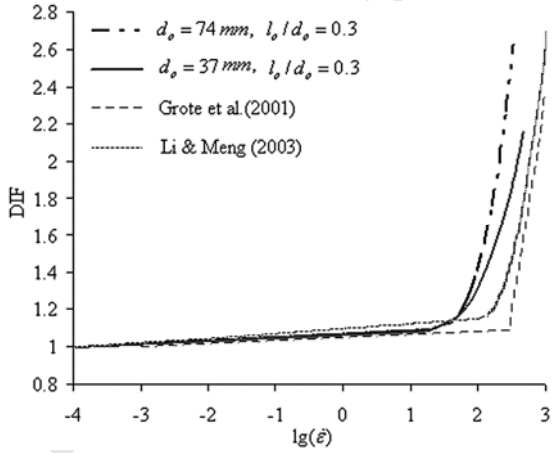

Fig.14. Comparison of the predicted DIF relations for specimen with different outer diameters.

Table 2 Parameters for solid mortar specimens with various outer diameters

	B_1	B_2	B_3	B_4	B_5	$\dot{\varepsilon}_t$ / s^{-1}
74 mm	0.0180	4	1.470	-4.511	4.588	22.9
37 mm	0.0161	4	0.684	-2.012	2.608	22.9
10.1~18.8 mm Grote et al. (2001)	0.0157	3	0.383	0.226	-1.765	266
12 mm Li & Meng (2003)	0.0258	4	1.729	-7.137	8.530	100

3.5 The effect of friction on DIF

Based on a comprehensive two-dimensional analysis, Bertholf and Karnes (1975) concluded that the friction effect could be effectively minimized if the ends of the metal specimen in an SHPB test are well lubricated. However, the friction coefficient of a concrete-like material specimen is normally larger than that of a metal specimen as its surface is much coarser than the surface of a metallic specimen, and thus, the friction effect may not be completely neglected even though the interface is lubricated. It is well known that SHPB results are particularly susceptible to the friction at the interface between the pressure bar and the specimen. Therefore, it is necessary to investigate the effect of friction on the measurement of the DIF of concrete-like materials in SHPB tests.

A series of parametric analyses using an FEM model with constant friction coefficients varying from 0 to 0.7 and a slenderness ratio of 0.5 have been performed for mortar specimens (Li and Meng 2003). It is shown that the DIF of mortar is enhanced considerably in an SHPB test when $\mu \geq 0.2$. The friction effect is another constraint to the lateral motion of the specimen, and the DIF due to this may also be misinterpreted as a strain-rate effect. On the other hand, the influence of the friction coefficient on DIF becomes insignificant when $\mu \leq 0.1$. The friction coefficient between the specimen and the pressure bars can be reduced to this value by applying lubrication properly and ensuring the smoothness of the specimen faces, which however is not always the case in practice.

In fact, the friction coefficient is not a constant, but varies with the relative velocity (sliding velocity) between two contacting surfaces. The kinetic friction coefficient is normally smaller than the static friction coefficient. In an SHPB test, when assuming the specimen to be incompressible, the maximum relative radial velocity on the interfaces between a tubular specimen and the end surfaces of the pressure bars can be estimated by

$$V = \frac{d_0 \dot{\varepsilon}}{4(1-\varepsilon)} \tag{14}$$

in which d_0 is the original outer diameter of the specimen, ε is strain and $\dot{\varepsilon}$ is strain-rate. Thus, for the tubular specimens of d_0 =74 mm and d_i =30.9 mm, Fig.15 shows the variation of the maximum relative radial velocity V on the outer surface of the specimen versus strain at different strain rates in SHPB tests. It can be seen that the specimen may slide on the end surfaces of pressure bars at velocity in the range of 0.62 m/s to 12 m/s for a common SHPB test when measured strain is less than 3.46%.

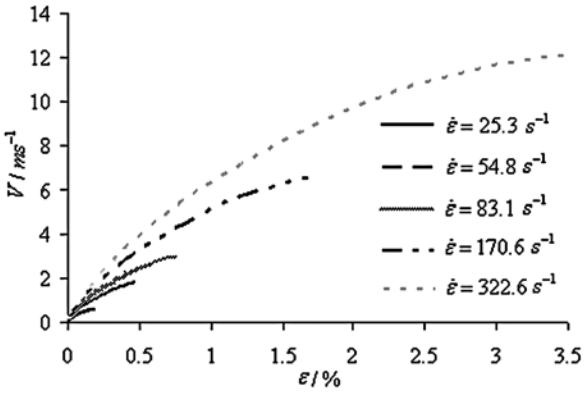

Fig.15.Variation of the maximum relative speed V with the axial strain in an SHPB test on a tubular mortar specimen.

In this velocity range, the so-called Stribeck curve is suitable to describe the variation of the friction coefficient with the relative velocity (Pavelescu and Tudor 1987). The friction coefficient has its maximum value at $V = 0$ (i.e., the static friction coefficient, μ_s) and then decreases considerably to its minimum value with the increase of the relative velocity in a small range and followed by a slow increase with the relative velocity. However, details of the relationship between the kinetic friction coefficient and the sliding velocity depend upon the degree of surface roughness and lubrication, e.g. as the longitudinal pressure is applied, the lubricant will be pressurized, which could squeeze it out from the interface and/or increase the pore pressure of a thin layer lubricant fluid on the specimen. Such effects could influence the local stress state, and therefore, affect the SHPB measurements. The effects of the hydrodynamics of lubricants in SHPB tests were partly addressed in Martins et al. (1990), Hess and Soom (1990) and Helouvry et al. (1994), which, however, demands further investigations.

In order to find the dependence of the kinetic friction coefficient on the sliding velocity in the velocity range of 0-12 m/s, a simple apparatus for the measurement of the kinetic friction coefficient at a velocity of several meters per second is set up as shown in Fig.16, which consists of a slip-way, a specimen and some measuring devices. A highly sensitive capacitive accelerometer on a ceramic base with built-in electronics is used in the test, which can measure acceleration down to 0 Hz. The contact surface is lubricated by Shell Helix Super oil to simulate a similar situation in a SHPB test. The specimen slips from the top of the slip-way. Using the data of the acceleration history $a(t)$, the dynamic coefficient of friction $\mu_d(t)$ between the specimen and the stainless steel slip-way and the corresponding velocity history $V(t)$ can be obtained using the following formula,

$$\mu_d(t) = \tan\theta - \frac{a(t)}{g\cos\theta}, \quad V(t) = \int_0^t a(t) \tag{15}$$

where θ is the slope angle of the slip-way, and g the acceleration of gravity.

A series of tests have been performed to construct the kinetic friction model between mortar and steel and between concrete and steel, and the results are shown in Fig.17, where the vertical coordinate is the ratio of the kinetic friction coefficient to the static friction coefficient, μ_d / μ_s, and the horizontal coordinate is V. In a practical numerical analysis, it is necessary to propose a simplified friction model to describe experimental results. Comparing with the Stribeck curve (Meng 2003), it is reasonable to use an exponential-linear function to fit the testing results, i.e.

$$\mu_d / \mu_s = \begin{cases} 1 & V = 0 \\ P_1 \exp(-V / P_2) + P_3 V + P_4 & V > 0 \end{cases} \tag{16}$$

in which $P_1 \sim P_4$ are constants obtained from the test results, as shown in Table 3.

It is seen that the kinetic friction coefficient fitted by an exponential-linear function is better than the bilinear function used in Meng (2003). Furthermore, it can be easily input into numerical simulations. The maximum relative velocity in the present tests (up to 4.57 m/s) covers the relative velocity range in typical SHPB tests of concrete-like materials because Eq.(14) is based on the incompressibility of the specimen and the neglect of Poisson's effect in the pressure bar material. When the deformation of an SHPB specimen is mainly elastic before the occurrence of failure and the lateral movement of the pressure bar are considered, the relative velocity between the specimen face and the pressure bar is smaller than that estimated by Eq.(14).

In order to study the friction effect on the SHPB results using the constant friction model and the proposed kinetic friction model, four cases were simulated with different values of μ, i.e., (1) μ=0, which corresponds to the frictionless case; (2) μ=0.163, corresponding to μ_d / μ_s=0.38, which is the minimum value of Eq.(16); (3) $\mu = \mu_d$ where μ_d is given by Eq.(16), which is implemented into ABAQUS using user subroutine VFRIC; (4) $\mu = \mu_s = 0.430$, which is the static friction coefficient. A simulation example of stress-strain response is shown in Fig.18 for the strain rate corresponding to ultimate strength of 170 s^{-1}. The maximum difference among Cases (1)-(3) is about 15%. However, a large difference between Case (4) and three other cases are observed.

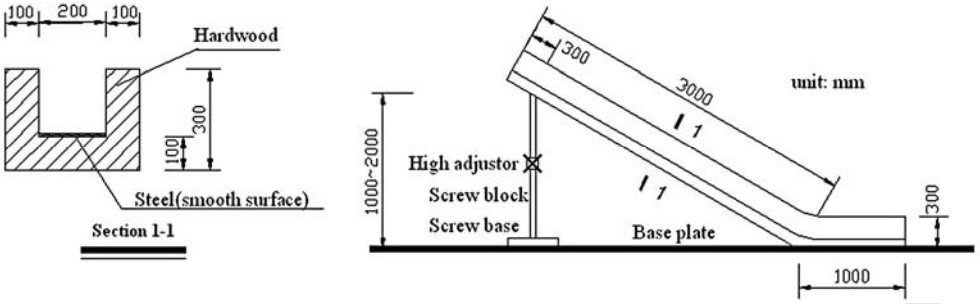

(a)

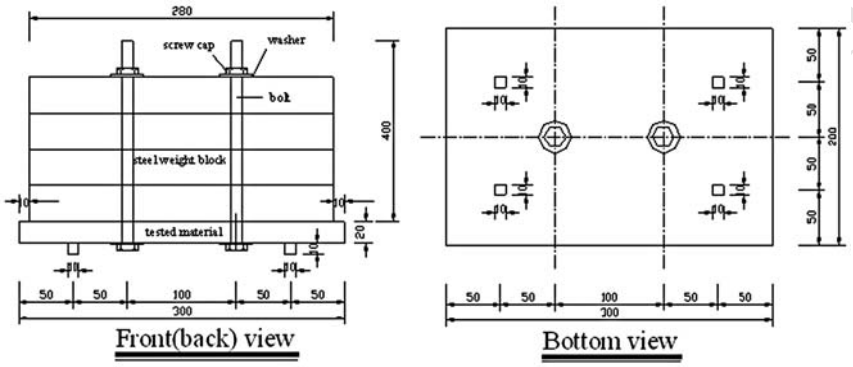

(b)

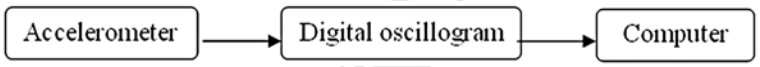

(c)

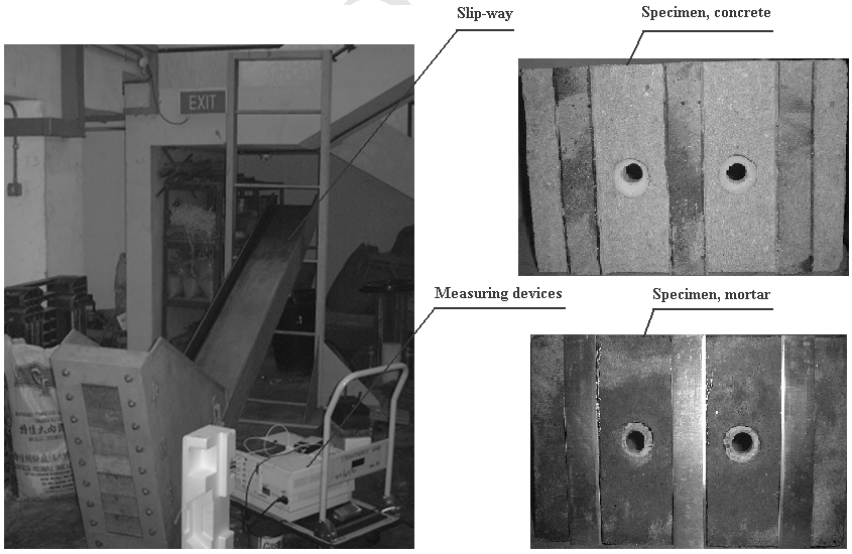

(d)

Fig.16. Test apparatus: (a) slip-way [side view]; (b) specimen; (c) measuring devices; (d) photo of the test apparatus.

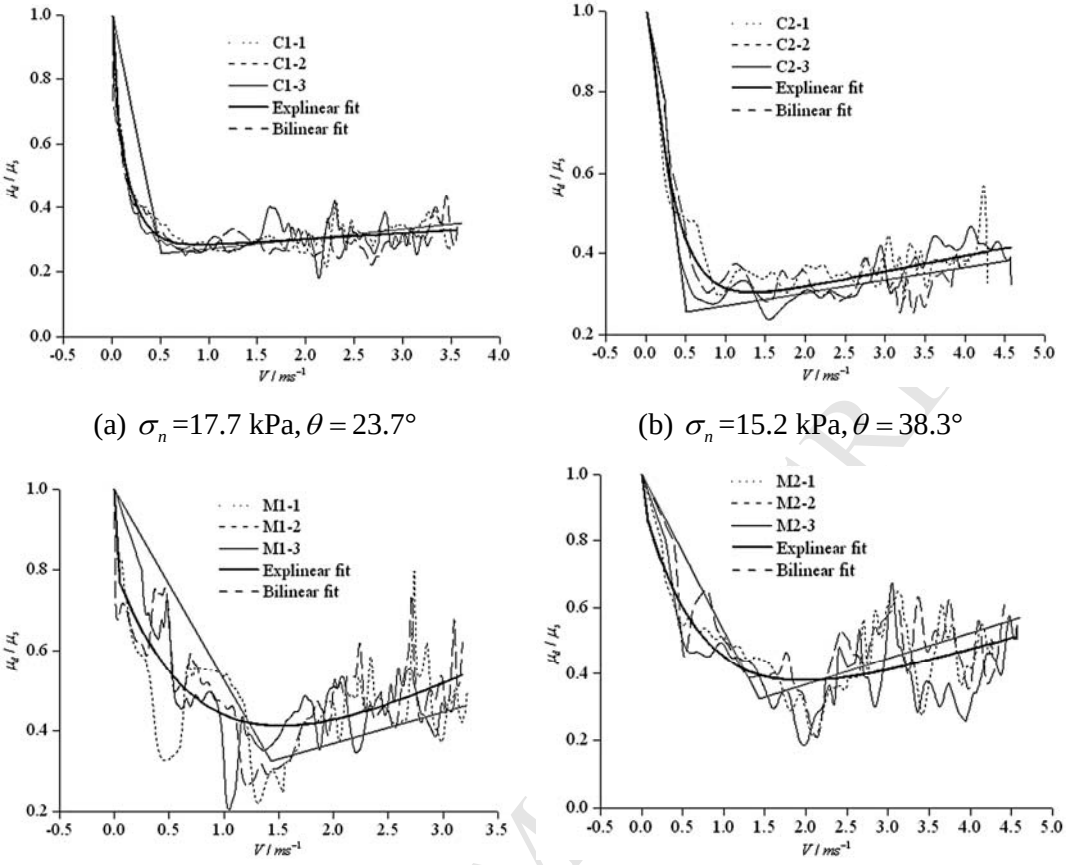

(a) σ_n =17.7 kPa, $\theta = 23.7°$ (b) σ_n =15.2 kPa, $\theta = 38.3°$

(c) σ_n =15.5 kPa, $\theta = 23.7°$ (d) σ_n =13.3 kPa, $\theta = 38.3°$

Fig.17. Variations of kinetic friction coefficient with relative velocity for (a) and (b) concrete specimens; (c) and (d) mortar specimens.

Table 3 Parameters in Eq.(16)

	P_1	P_2	P_3	P_4
Concrete	0.697	0.246	0.255	0.0285
Mortar	0.720	0.780	0.145	0.102

A constant friction coefficient of zero and the kinetic friction model are applied in the finite element analysis of SHPB tests for tubular mortar specimens of d_0 =74 mm and d_i =30.9 mm. As shown in Fig.19, the DIFs from SHPB simulations when using the kinetic friction model is generally greater than those predicted based on the frictionless assumption in the strain-rate range of 10^1-10^3 s^{-1}, especially when the strain-rate is greater than the transition strain-rate. The transition strain-rate is increased when friction is neglected. Thus a more reliable assessment and correction procedure for SHPB tests should be based on the kinetic friction model whenever the results of kinetic friction coefficient versus relative velocity are

available.

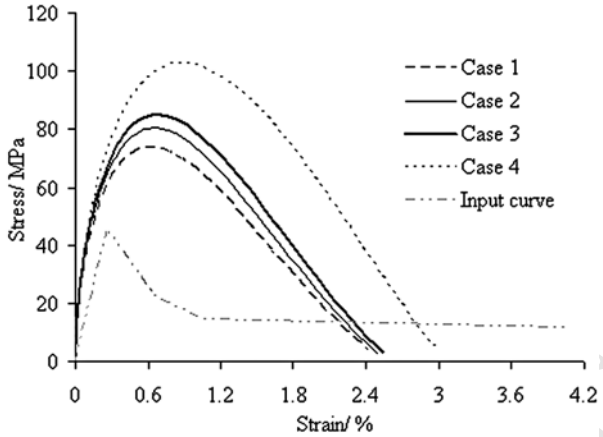

Fig.18. Comparison of calculated stress-strain relations for different friction models at the strain rate corresponding to ultimate strength of 170 s^{-1}.

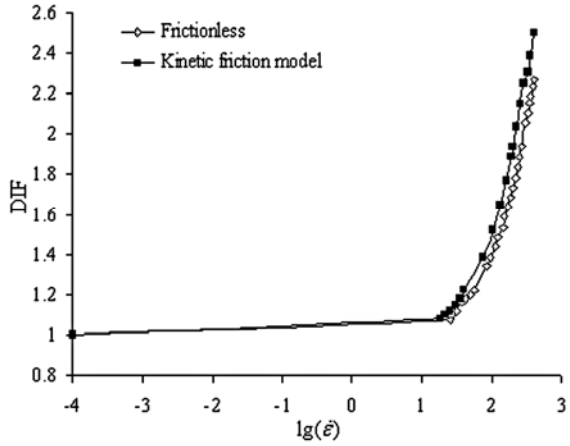

Fig.19. Contribution of friction to the dependence of the DIF on strain-rate in the numeric SHPB tests when using different friction models.

4 Conclusions

A series of numerical simulations of SHPB tests were performed on solid and tubular cylindrical mortar specimens. The influences of residual strength, specimen geometries and friction on the DIF of mortar samples are demonstrated. It shows that tubular specimen can reduce the radial confinement effects and the apparent DIFs measured for tubular specimens are smaller than those for solid ones at the same strain-rate.

Friction on the interface between pressure bars and SHPB specimen is another possible source of error for SHPB tests and should be examined through numerical analyses. Based on

kinetic friction tests and numerical simulations, it was found that the difference between the constant friction model and the kinetic friction model may lead to different results. Therefore, whenever possible, a more reliable assessment and correction procedure should be based on a kinetic friction model.

Finally, the present study supports the discovery in Li and Meng (2003) that the apparent DIF is a kind of pseudo strain-rate effects caused by radial confinement introduced by axial strain acceleration, small aspect ratio and friction constrains, which should be corrected before it is used in the design and numerical models. Otherwise, non-conservative results will be produced, which may lead to dangerous designs of the protective structures against impact and blast loads. Furthermore, the conclusions obtained in this study may be applicable to other concrete-like materials tested in similar conventional SHPB configurations because the normalized DIF-$\lg(\dot{\varepsilon})$ curves are found to be authentically insensitive to the value of the quasi-static unconfined compressive strength.

Acknowledgements: First author acknowledges the support from the open funding programme (KFJJ05-3) from State Key Laboratory of Explosion Science and Technology. Second author acknowledges the studentship from the School of Mechanical, Aerospace and Civil Engineering, The University of Manchester and the scholarship from Henry Lester Trust.

References

ABAQUS Theory Manual, version 6.5, 2004. Hibbitt, Karlson & Sorensen, Inc.

Abrams, D.A., 1917. Effect of rate of application of load on the compressive strength of concrete. Proc. Amer. Soc. Test. Mater. 17(2), 364-377.

Bertholf, L.D., Karnes, C.H., 1975. Two dimensional analysis of the split Hopkinson pressure bar system. J. Mech. Phys. Solids 23, 1-19.

Bischoff, P.H., Perry, S.H., 1991. Compression behavior of concrete at high strain-rates. Mater. Struct. 24, 425-450.

Brace, W.F.., Jones, A.H., 1971. Comparison of uniaxial deformation in shock and static loading of three rocks. J. Geophys. Res. 76, 4913-4921.

Comite Euro-International du Beton, 1993. CEB-FIP model code 1990, Redwood Books, Trowbridge, Wiltshire, UK.

Dahl, K.K.B., 1992. A failure criterion for normal and high strength concrete, no. R-286. Department of Structural Engineering, Technical University of Denmark.

Davies, E.D.H., Hunter, S.C., 1963. The dynamic compression testing of solids by the method

of the split Hopkinson bar. J. Mech. Phys. Solids 11, 155-179.

Dioh, N.N., Leevers, P.S., Williams, J.G., 1993. Thickness effects in split Hopkinson pressure bar tests. Polym 34, 4230-4234.

Field, J.E., Walley, S.M., Proud, W.G., Goldrein H.T., Siviour, C.R., 2004. Review of experimental techniques for high rate deformation and shock studies. Int. J. Impact Eng. 30, 725-775.

Forrestal, M.J., Wright, T.W., Chen, W., 2007. The effect of radial inertia on brittle samples during the split Hopkinson pressure bar test. Int. J. of Impact Eng. 34, 405-411.

Fu, H.C., Erki, M.A., Seckin, M., 1991a. Review of effects of loading rate on concrete in compression. ASCE J. Struct. Eng. 117, 3645-3659.

Fu, H.C., Erki, M.A., Seckin, M., 1991b. Review of effects of loading rate on reinforced concrete. ASCE J. Struct. Eng. 117, 3660-3679.

Gorham, D.A., Pope, P.H., Cox, O., 1984. Sources of error in very high strain rate compression tests. Inst. Phys. Conf. Ser. 70, 151-158.

Gorham, D.A., 1989. Specimen inertia in high strain-rate compression. J. Phys. D: Appl Phys. 22, 1888-1893.

Gorham, D.A., 1991. An effect of specimen size in the high strain rate compression test. J. Phys. IV. France 1(C3), 411-418.

Gorham, D.A., Pope, P.H., Field, J.E., 1992. An improved method for compressive stress-strain measurements at very high strain rates. Proc. R. Soc. Lond. A 438, 153-170.

Grote, D.L., Park, S.W., Zhou, M., 2001. Dynamic behavior of concrete at high strain-rates and pressures: I. Experimental characterization. Int. J. Impact Eng. 25, 869-886.

Haddow, J.B., 1965. On compression of thin disk. Int. J. Mech. Sci. 7, 657-660.

Helouvry, B.A., Dupont, P., Wit, C.C.D., 1994. A survey of models, analysis tools and compensation methods for the control of machines with friction. Automatica 30, 1083-1138.

Hess, D.P., Soom, A., 1990. Friction at a lubricated line contact operating at oscillating sliding velocities. J. Tribol. 112, 147-152.

Kolsky, H., 1949. An investigation of the mechanical properties of materials at very high rates of loading. Proc. Phys. Soc. London (B) 62, 676-700.

Li, Q.M., Meng, H., 2003. About the dynamic strength enhancement of concrete-like materials in a split Hopkinson pressure bar test. Int. J. Solids Struct. 40, 343-360.

Maher, A., Darwin, D., 1980. Mortar constituent of concrete in compression, ACI J., 100-109.

Malvar, L.J., Crawford, J.E., Wesevich, J.W., Simons, D., 1997. A plasticity concrete material model for DYNA3D. Int. J. Impact Eng. 19, 847-873.

Malvern, L.E., Ross, C.A., 1985. Dynamic response of concrete and concrete structures,

Second Annual Technical Report, AFOSR contract no. F49620-83-K007.

Martins, J.A.C., Oden, J.T., Simoes, F.M.F., 1990. A study of static and kinetic friction. Int. J. Eng. Sci. 28, 29-92.

Meng, H., 2003. Numerical split Hopkinson pressure bar (NSHPB) test and its applications in the assessment and improvement of SHPB test results. PhD dissertation. Nanyang Technological University, Singapore.

Meng, H., Li, Q.M., 2003. Correlation between the accuracy of a SHPB test and the stress uniformity based on numerical experiments. Int. J. Impact Eng. 28, 537-555.

Park, S.W., Xia, Q., Zhou, M., 2001. Dynamic behavior of concrete at high strain rates and pressures: II. Numerical simulation. Int. J. Impact Engng. 25, 887-910.

Pavelescu, D., Tudor, A., 1987. The sliding friction coefficient-its evolution and usefulness. Wear 120, 321-336.

Ross, C.A., Thompson, P.Y., Tedesco, J.W., 1989. Split-Hopkinson pressure-bar tests on concrete and mortar in tension and compression. ACI Mater. J. 86, 475-481.

Ross, A., Tedesco, J.W., Kuennen, S.T., 1995. Effects of strain rate on concrete strength. ACI Mater. J. 92, 37-47.

Ross, A., Jerome, D.M., Tedesco, J.W., Hughes, M.L., 1996. Moisture and strain rate effects on concrete strength. ACI Mater. J. 93, 293-300.

Samata, S.K., 1971. Dynamic deformation of aluminum and copper at elevate temperature. J. Mech. Phys. Solids 19, 117-122.

Tedesco, J.W., Powell, J.C., Ross, C.A., Hughes, M.L., 1997. A strain-rate-dependent concrete material model for ADINA. Comput. Struct. 64, 1053-1067.

Tedesco, J.W., Ross, C.A., 1998. Strain-rate-dependent constitutive equations for concrete. ASME J. Press. Vessel Technol. 120, 398-405.

Williams, M.S., 1994. Modeling of local impact effects on plain and reinforced concrete. ACI Struct. J. 91, 178-187.

Zhang, J.G., 2001. Triaxial Behaviour of Cement Mortar Under Monotonic Loading, Master Thesis. Nanyang Technological University, Singapore.

Zhang M., Wu H.J., Li Q.M., Huang F.L., 2009. Further investigation on the dynamic compressive strength enhancement of concrete-like materials based on split Hopkinson pressure bar tests Part I: Experiments. Int J. Impact Engng..